Colloids and Surfaces B: Biointerfaces 144 (2016) 222–228

Colloids and Surfaces B: Biointerfaces

journal homepage: www.elsevier.com/locate/colsurfb

New evidence for Cu-decorated binary-oxides mediating bacterial inactivation/mineralization in aerobic media

S. Rtimi [a], C. Pulgarin [a,*], M. Bensimon [b], J. Kiwi [a,*]

[a] Ecole Polytechnique Fédérale de Lausanne, EPFL-SB-ISIC-GPAO, Station 6, CH-1015, Lausanne, Switzerland
[b] Ecole Polytechnique Fédérale de Lausanne, EPFL-ENAC-IIEGR-CEL, Station 18, CH-1015, Lausanne, Switzerland

ARTICLE INFO

Article history:
Received 26 December 2015
Received in revised form 23 March 2016
Accepted 24 March 2016
Available online 6 April 2016

Keywords:
Binary-oxides
Oxidative radicals
Potential surface shifts
Bacteria mineralization
FTIR-peak shifts

ABSTRACT

Binary oxide semiconductors TiO_2-ZrO_2 and Cu-decorated TiO_2-ZrO_2 (TiO_2-ZrO_2-Cu) uniform films were sputtered on polyester (PES). These films were irradiated under low intensity solar simulated light and led to bacterial inactivation in aerobic and anaerobic media as evaluated by CFU-plate counting. But bacterial mineralization was only induced by TiO_2-ZrO_2-Cu in aerobic media. The highly oxidative radicals generated on the films surface under light were identified by the use of appropriate scavengers. The hole generated on the TiO_2-ZrO_2 films is shown to be the main specie leading to bacterial inactivation. TiO_2-ZrO_2 and Cu-decorated TiO_2-ZrO_2 films release Zr and Ti <1 ppb and Cu 4.6 ppb/cm^2 as determined by inductively coupled plasma mass spectrometry (ICP-MS) This level is far below the citotoxicity permitted level allowed for mammalian cells suggesting that bacterial disinfection proceeds through an oligodynamic effect. By Fourier transform attenuated infrared spectroscopy (ATR-FTIR) the systematic shift of the predominating $\nu_s(CH_2)$ vibrational-rotational peak making up most of the bacterial cell-wall content in C was monitored. Based on this evidence a mechanism suggested leading to C—H bond stretching followed by cell *lysis* and cell death. Bacterial inactivation cycling was observed on TiO_2-ZrO_2-Cu showing the stability of these films leading to bacterial inactivation.

1. Introduction

Resistance of bacteria to antibiotics is a serious health problem leading specially during the last decade to an increase in the hospital-acquired infections (HAI). Therefore, the development of innovative antibacterial surfaces presenting long-term effective operational lifetimes, biocompatibility and mechanical resistance is a timely research subject. Antibacterial Cu-colloids have been reported during the last 3 decades showing their antibacterial activity [1]. Bacteria, yeasts, and viruses have been abated on metallic copper surfaces, and the term "contact killing" has been coined for this process. The use of copper has shown a potential antibacterial response in health care settings. Contact killing was observed to take place at a rate of at least 7–8 logs per hour, and no live microorganisms were recovered from copper surfaces after prolonged incubation. Copper has recently been registered at the U.S. Environmental Protection Agency as the first solid antimicrobial material. Cu-cell have been shown to damage the cell envelope through the release of Cu-ions. [2]. Recent work has shed light on mechanistic aspects of contact killing. These findings will be reviewed here and juxtaposed with the toxicity mechanisms of ionic copper. The merit of copper as a hygienic material in hospitals has been extensively reported to preclude/decrease viral, nosocomial infections caused by antibiotic resistant bacteria by textile fabrics impregnated by colloidal Cu by Borkow and Gabbay [3]. More recently Cu-ions have been reported to be biocidal binding to specific sites in the DNA-phosphate destroying the DNA double helix or damaging the bacterial cell wall. The cell wall envelope proteins and lipids were damaged by contact with Cu-surfaces, but the contact killing was not necessarily related to lethal damages to the DNA. When the bacterial cell wall is damaged, the Cu-ions enter the cytoplasm causing metabolical disruption [4].

Sol-gel commercial preparations using Ag have been widely reported during the last few years. These sol-gel suspensions were subsequently annealed on heat resistant substrates [6]. But the thicknesses of these Ag-films and in some cases of Cu-films were not reproducible, they were not mechanically stable, they exhibited low adhesion and could be wiped off by a cloth or by hand contact [6]. The colloid deposition on substrates require temperatures of few hundred degrees for an adequate adherence to the

* Corresponding authors. Tel.: +41 216936150.
E-mail addresses: john.kiwi@epfl.ch, cesar.pulgarin@epfl.ch (J. Kiwi).

http://dx.doi.org/10.1016/j.colsurfb.2016.03.072
0927-7765/

substrate and this will not work on low thermal resistant substrates like PES. This moved us to work on the preparation of sputtered antibacterial films to overcome the shortcomings of colloidal loaded films and this is one of the main points addressed in this study.

This study reports new findings by TiO_2-ZrO_2 and TiO_2-ZrO_2-Cu films on PES following our first study on these materials [7]. These materials were reported recently as catalysts and for their use in optical/electronic devices. The films were reported by sol-gel and later calcined on substrates resisting higher temperatures [8,9]. By inductively coupled plasma mass-spectrometry (ICP-MS) we will show that the TiO_2-ZrO_2 and Cu decorated TiO_2-ZrO_2 release Ti, Zr and Cu at ppb levels far below the amounts permitted by sanitary regulations and therefore they can be used safely as antibacterial agents in a mammalian cell context [10,11]. The low level found for Ti and Cu also suggests that the *Escherichia coli* disinfection occurs through an oligodynamic effect [12,13]. The present study addresses new features for films activated by low intensity solar light leading to bacterial inactivation compared to other antibacterial films [14,15]. The bacterial inactivation/mineralization in aerobic media is reported and the identification of the $OH^{\bullet}$-radical was determined quantitatively. A bacterial inactivation mechanism is suggested based on the ATR-FTIR spectroscopic and other experimental data found during this study.

2. Experimental

2.1. Preparation of binary oxides films by sputtering, quantitative analysis of the film content by X-ray fluorescence (XRF) and CO_2 measurements

Thin Ti and Zr films were sputtered on PES by direct current magnetron sputtering (DCMS) at 200 mA and 300 V in a reactive oxygen atmosphere using a mixed target of Ti and Zr (50%–50%) obtained from K. Lesker, Hastings, UK. The substrate-to-target distance was 10 cm and targets were 2 inches in diameter. Cu sputtering on the TiO_2-ZrO_2 layers was applied for times up to 10 s. The PES used was Dacron, type 54 spun, plain weave ISO 105-F04 (EMPA) used for color fastness determinations. The nominal thickness calibration of the TiO_2-ZrO_2 films was carried out on Si-wafers with a profilometer (Alphastep500, TENCOR). CO_2 was monitored using a micro-GC 3000 (Agilent Technologies) provided with a PoraPlot U 8 m column using He as carrier gas.

2.2. CFU counting, irradiation procedures and ICP-MS determination of the Ti, Zr and Cu released during bacterial inactivation

Escherichia coli (*E. coli K12* ATCC23716 from Atlas Heraeus GmbH, Hananu, DE) on 2 cm by 2 cm sputtered samples were placed into a Petri glass-dish and irradiated in the cavity of Suntest solar simulator cavity tuned at (50 mW/cm^2). 100 μL culture aliquots with an initial concentration of ~10^6 colony forming units (CFU/mL) in NaCl/KCl (pH 7) were placed on the samples. After pre-selected irradiation times, the samples were transferred into a sterile 2 mL Eppendorf tube containing 1 mL autoclaved NaCl/KCl saline solution. This solution was subsequently mixed thoroughly using a Vortex for 3 min. Serial dilutions were made in NaCl/KCl solution. Samples of 100-μL were pipetted onto a nutrient agar plate and then spread over the surface of the plate using standard plate method. Agar plates were incubated lid down, at 37 °C for 24 h before counting. Three independent assays were done for each sputtered sample. The TiO_2-ZrO_2 films (with and without Cu) were kept in a sterile oven at 60 °C to avoid contamination prior to the bacterial testing. The 100-μL bacteria samples were then uniformly distributed on the samples. A cut-off filter was inserted in the irradiating cavity to block the light below 310 nm. Agar was purchased from Merck GmbH, Microbiology division KGaA under the catalogue N° 1.05463.0500. The CFU statistical analysis was performed calculating the standard deviation values (SD, σ = 5%).

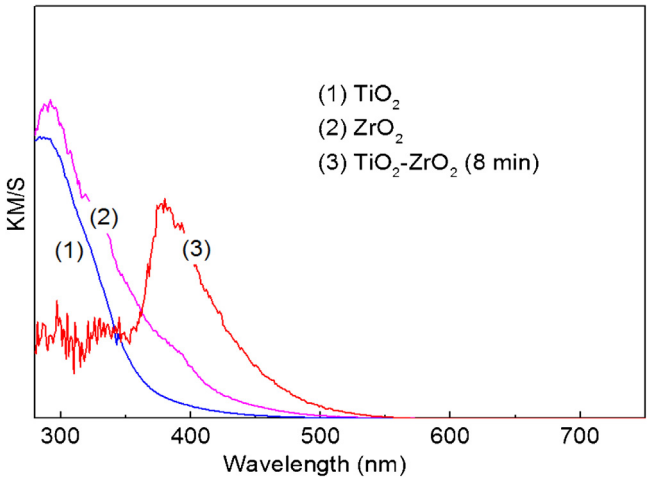

Fig. 1. Diffuse reflectance spectroscopy of (1) TiO_2, (2) ZrO_2 and (3) TiO_2-ZrO_2 sputtered for 8 min.

Determination by inductively coupled-plasma mass-spectrometry (ICP-MS) of Ti, Zr and Cu-ions was carried out by way of a Finnigan TM ICPS unit equipped with a double focusing reverse geometry mass spectrometer with an extremely low background signal and a high ion-transmission coefficient. The TiO_2, ZrO_2 and Cu/Cu-oxides and the washing solution were digested with nitric acid 69% (HNO_3:H_2O = 1:1) to remove organics in solution and to guarantee that there were no remaining ions adhered to the flask wall. The samples droplets are introduced to the ICP-MSunit trough a peristaltic pump to the nebulizer chamber allowing the sample components evaporation and ionization. The Ti, Zr and Cu found in the nebulizer droplets were subsequently quantified by mass spectrometry (MS).

2.3. Monitoring the local pH and interfacial potential shift during bacterial inactivation and quantitative detection of the bacterial inactivation by the generation of CO_2

The local-pH shifts and interfacial potentials were followed by means of a Jenco 6230 N (pH/mV/temperature meter) with a handheld microprocessor in splash proof case with 3 points calibration. The device can be monitored via RS-232-C IBM compatible communication interface and BNC, pH/ORP connector with 8-pin DIN ATC connector. To follow the bacterial mineralization induced under simulated solar light on the ZrO_2/PES, TiO_2/PES and TiO_2-ZrO_2-Cu PES films, the films were introduced in a 60 cc Pyrex flask and the CO_2 evolved was followed in a GowMac GC head provided for with a Poropak column using He as carrier gas. For the anaerobic experiments the flask was previously flushed with Ar gas.

2.4. Infrared spectroscopy (ATR-FTIR)

FTIR spectra were measured in a Portmann Instruments AG spectrophotometer equipped with a Specac attachment (45° one pass diamond crystal). Spectra were taken by 256 scans with a resolution of 2 cm^{-1} in the range 900–4000 cm^{-1}. The position of the IR peaks was found by the second derivative of the spectra after Fourier deconvolution.

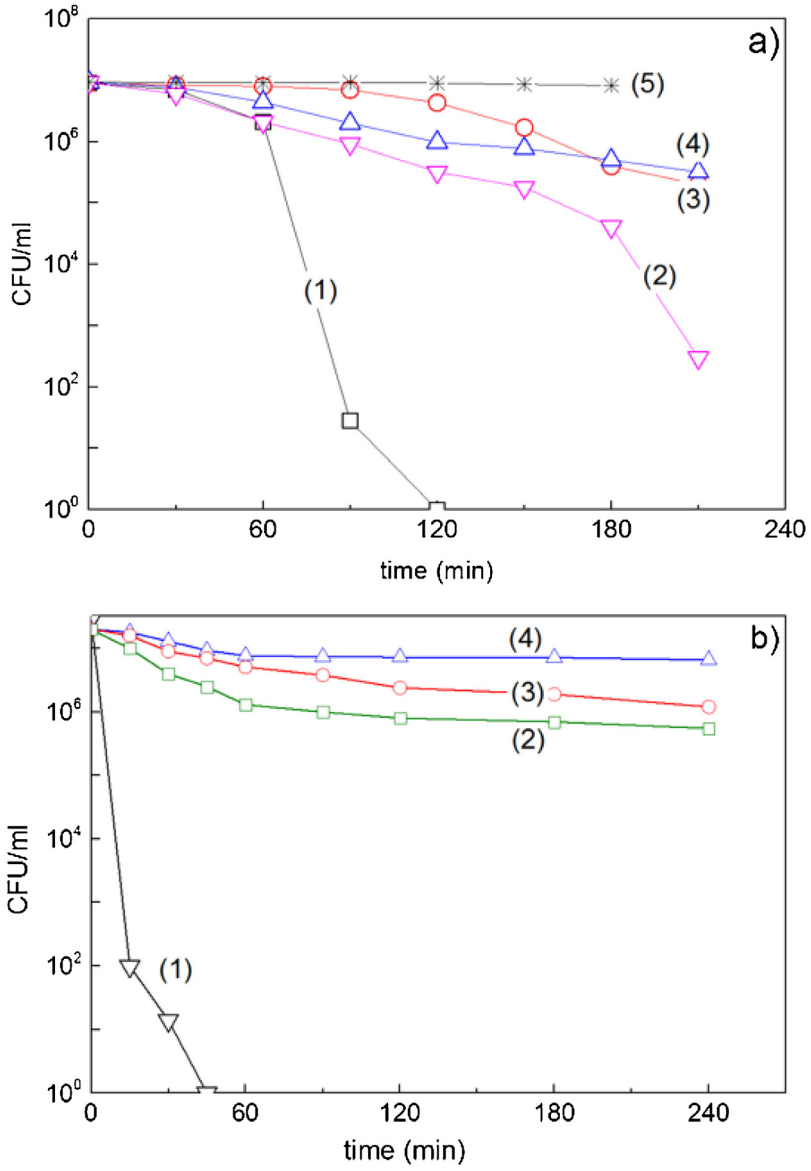

Fig. 2. (a) Trace (1) *E. coli* inactivation on TiO_2-ZrO_2 PES sputtered for 8 min under low intensity solar simulated light irradiation (50 mW/cm^2); trace (2) *E. coli* monitored as in trace (1) but adding 2 mM EDTA-2Na; trace (3) run as in trace (1) but adding 2 mM DMSO and finally trace (4) run as in trace (1) adding 2 mM SOD and finally trace (5) PES alone under solar simulated light irradiation (50 mW/cm^2). (b) (*E. coli* inactivation under low intensity solar simulated light irradiation (50 mW/cm^2) on: (1) TiO_2-ZrO_2/Cu PES sputtered for (8 min/10 s); (2) TiO_2-ZrO_2/Cu (8 min/10 s) + 2 mM SOD (3) TiO_2-ZrO_2/Cu (8 min/10 s) + 2 mM DMSO, and (4) TiO_2-ZrO_2/Cu (8 min/10 s) + 2 mM EDTA-2Na. Light solar simulated light irradiation (50 mW/cm^2). Error bars: SD, $\sigma = 5\%$.

3. Results and discussion

3.1. DRS of TiO_2-ZrO_2 and scavenging of the radicals generated by TiO_2-ZrO_2 and TiO_2-ZrO_2-Cu under light irradiation

Fig. 1 shows the diffuse reflectance spectra of TiO_2, ZrO_2 and TiO_2-ZrO_2 composites sputtered films for 8 min on PES. It is readily seen that the TiO_2-ZrO_2 spectrum in Fig. 1 presents a different spectrum compared to the TiO_2 and ZrO_2. This effect is due to networking in the binary oxide TiO_2-ZrO_2 but a definitive structure for this composite has not been reported [7–9]. Rtimi et al., have reported recently lower bacterial inactivation kinetics by TiO_2 and ZrO_2 each by itself when compared to the co-sputtered TiO_2-ZrO_2 binary-oxides [7]. The XRF determination of weight% of TiO_2 and ZrO_2 revealed 0.47 wt%/wt PES for a TiO_2-ZrO_2 sample sputtered for 8 min. Sputtering TiO_2-ZrO_2 for 6 min led to lower concentrations of TiO_2 and ZrO_2. These samples contained insufficient TiO_2 and ZrO_2 to induce fast bacterial inactivation kinetics. Samples sputtered for 12 min showed also a slower bacterial inactivation kinetics compared to TiO_2-ZrO_2 sputtered for 8 min. This can be attributed to the charge transfer/transport limited by the size of the grains and the increased thickness of the TiO_2-ZrO_2 layers affecting the diffusion of the generated charges under light in the TiO_2-ZrO_2-PES. This aspect will not be investigated further in the present study.

Fig. 2a, trace (1) shows the bacterial inactivation within 120 min on the TiO_2-ZrO_2-PES (8 min/10 s) sputtered samples. To sort out the relative contribution of the intermediate radicals generated at the TiO_2-ZrO_2 surface under low intensity sunlight, leading to the bacterial inactivation radical scavengers were added. Fig. 2, trace 2) shows the effect of ethylene diamine-tetraacetic acid disodium salt (EDTA-2Na) 2 mM solution a well-known TiO_2vb hole scavenger [9]. Fig. 2a, trace (3) shows the effect of the $OH^{\bullet}$ scavenger dimethyl-sulfoxide (DMSO) 2 mM solution. Next, Fig. 2a, trace 4) shows the effect of addition of superoxide-dismutase (SOD 2 mM)

an $O_2^{\circ -}$/superoxide scavenger. Fig. 2, trace (4) shows that SOD a strong (O_2^-) quencher inhibited to a great extent the bacterial inactivation on the TiO_2-ZrO_2 film. Fig. 2, trace 5) shows the negligible bacterial inactivation when PES was Suntest irradiated. The CFU/ml concentration decreased only marginally within 4 h in the dark.

Fig. 2b, trace (1) shows the bacterial inactivation on the TiO_2-ZrO_2-Cu films. Traces (2), (3) and (4) report the results of the inactivation kinetics when adding: (2) SOD an O_2^- scavenger: (3) DMSO and OH•-scavenger and finally (4) EDTA-2Na a hole (h^+) scavenger. The overall scavenging of the radicals using the same amount of scavengers led to a more significant quenching of the intermediate radicals compared to the runs reported in Fig. 2a. The vb hole (h^+) scavenged by EDTA-2Na turned out to be the most effective species precluding bacterial inactivation. EDTA has been reported to be a copper and zirconia chelator. To verify whether the activity is mainly from the photo-generated hole or due to the leached Cu, we carried out the bacterial inactivation experiment in the presence of bathocuproine disulfonate. No effect was observed upon addition of bathocuproine disulfonate on the bacterial inactivation kinetics under solar irradiation (50 mW/cm^2). This can be explained by the small amount of Cu-released during bacterial inactivation.

The band-gaps of the sputtered films were determined using the well-known Tauc's method [16] for TiO_2 (3.04 eV) and for ZrO_2 (2.96 eV). These band gaps were higher compared to the band-gaps of TiO_2-ZrO_2 (2.47 eV) and TiO_2-ZrO_2—Cu (2.25 eV). Therefore, a larger amount of the visible photons will be absorbed by TiO_2-ZrO_2 from the solar simulated light in the UV-region compared to either of the two oxides by themselves.

The TiO_2-ZrO_2-Cu was shown in Fig. 2b, trace 1) to accelerate drastically the bacterial inactivation kinetics compared to TiO_2-ZrO_2 shown in Fig. 2a, trace 1). This may be ascribed to the narrower band of TiO_2-ZrO_2-Cu. Cu has been found to introduce narrowing in the TiO_2-ZrO_2 band-gap (2.25 eV) by a mechanism that has not been reported yet due to the extremely low quantities of Cu decorating the TiO_2-ZrO_2 samples (ppb-range) as shown in Table 1. No doping by Cu takes place in the TiO_2-ZrO_2–PES film since the Cu in found in the ppb range was too low to induce a doping effect. For this reason, no evidence in the XRD-spectrogram was found for the Cu (XRD spectrogram not shown).

3.2. Evidence for bacterial mineralization under light irradiation in aerobic but not in anaerobic media

Fig. 3a, traces 1,2 presents the low CO_2 generation during bacterial inactivation photocatalyzed by TiO_2-PES and ZrO_2-PES. A slightly higher amount of CO_2 was generated by TiO_2-ZrO_2 films in aerobic media as reported in Fig. 3a, trace 3. Fig. 3b, trace 1 presents the significant *E. coli* mineralization on TiO_2-ZrO_2-Cu film in aerobic media. Fig. 3b, traces (2–4) show that in the absence of O_2 (air) in the dark precludes bacterial mineralization. These results will be further discussed in Section 3.3 below describing the local pH and surface potential changes in aerobic/anaerobic media during the bacterial inactivation in the dark and under light.

Table 1
Atomic release during PES-TiO_2-ZrO_2 and PES-TiO_2-ZrO_2/Cu recycling leading to bacterial inactivation detected by inductively coupled plasma mass spectrometry (ICP-MS).

		Ti (ppb)	Zr (ppb)	Cu (ppb)
TiO_2-ZrO_2/Cu	Cycle 1	<1	0.8	13.6
	Cycle 3	<1	0.2	5.9
	Cycle 5	<1	0.1	4.6
TiO_2-ZrO_2	Cycle 1	<1	<1	–
	Cycle 3	<1	<1	–
	Cycle 5	<1	<1	–

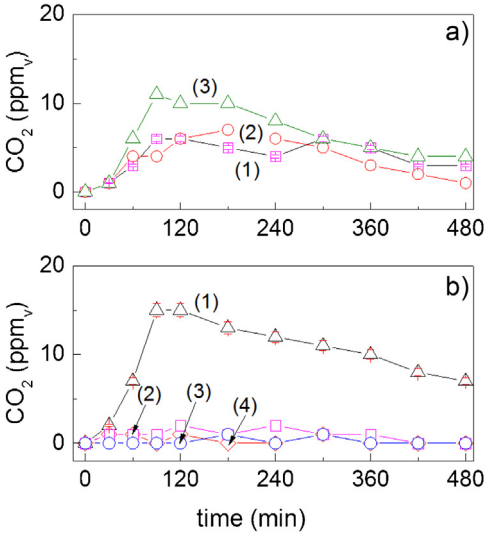

Fig. 3. (a) CO_2 production during bacterial inactivation by the films (1) TiO_2/PES sputtered for 8 min, (2) ZrO_2/PES sputtered for 8 min and (3) TiO_2-ZrO_2/PES sputtered for 8 min. Light source: solar simulated light irradiation (50 mW/cm^2). (b) CO_2 production during bacterial inactivation by the films: (1) TiO_2-ZrO_2/Cu/PES sputtered for 8 min/10 s under aerobic conditions/light irradiation, (2) TiO_2-ZrO_2/Cu/PES sputtered for 8 min/10 sunder anaerobic conditions/light irradiation, (3) TiO_2-ZrO_2/Cu/PES sputtered for 8 min/10 s under aerobic conditions/in the dark and (4) TiO_2-ZrO_2/Cu/PES sputtered for 8 min/10 s under anaerobic conditions in the dark. Error bars: SD, $\sigma = 5\%$.

3.3. Local pH-changes and surface potential evolution in the dark and under light

Fig. 4a presents the local pH-shift at the TiO_2-ZrO_2-Cu/PES interface in the dark within the bacterial inactivation time. A pH-decrease between 7.0 and pH 6.6 was observed within 2400 s or 45 min. This pH shift is equivalent to a fourfold increase in the concentrations of H^+. This pH change is due to short chain carboxylic acids (branched or not) generated in solution during the bacterial inactivation process presenting with pK_a values around~3 [5]. Fig. 4a shows that after 2400 s, the pH values recover up to pH ~6.7 due to the elimination of short carboxylic acids through mineralization of the C-intermediates compounds to CO_2. This is the final step in the bacterial mineralization by TiO_2 photocatalysis for many organic compounds and dyes [5,17]. Fig. 4a shows a pH-recovery step in the dark, but the recovery presented smaller amplitudes with values between pH's 6.6 and 7.6. The CO_2 generation under light in aerobic media, is a typical a photo-Kolbe CO_2 elimination reaction as shown below (1) [18].

$$RCOO\text{-} + TiO_2\text{-}ZrO_2\text{-}Cu/PES + h\nu \rightarrow R^{\circ} + CO_2 \quad (1)$$

Fig. 4b shows a significant steeper pH-decrease during the time of bacterial inactivation followed by a steep recovery to the initial pH. A much larger pH change is induced by TiO_2-ZrO_2-Cu/PES under light irradiation compared to runs in the dark reported in Fig. 4a. This points to the necessity of light activation to generate CO_2. A significant elimination of CO_2 occurs through a photo-Kolbe reaction as shown in Fig. 3b, trace 1 [18,19].

The interface potential on the TiO_2-ZrO_2-Cu PES film decreases during dark bacterial oxidation as shown in Fig. 4a, due to the increase in the bacterial cell wall permeability leading to damage of the cell wall. The increase in cell wall permeability leads to loss of the barrier function to control exchange of ions in and out of the cell cytoplasm [20,21].

The results reported in Fig. 4a and Fig. 4b have shown a pH shift to more acidic values within the bacterial inactivation period. This observation can be related to Fig. 2a and b showing the bacterial

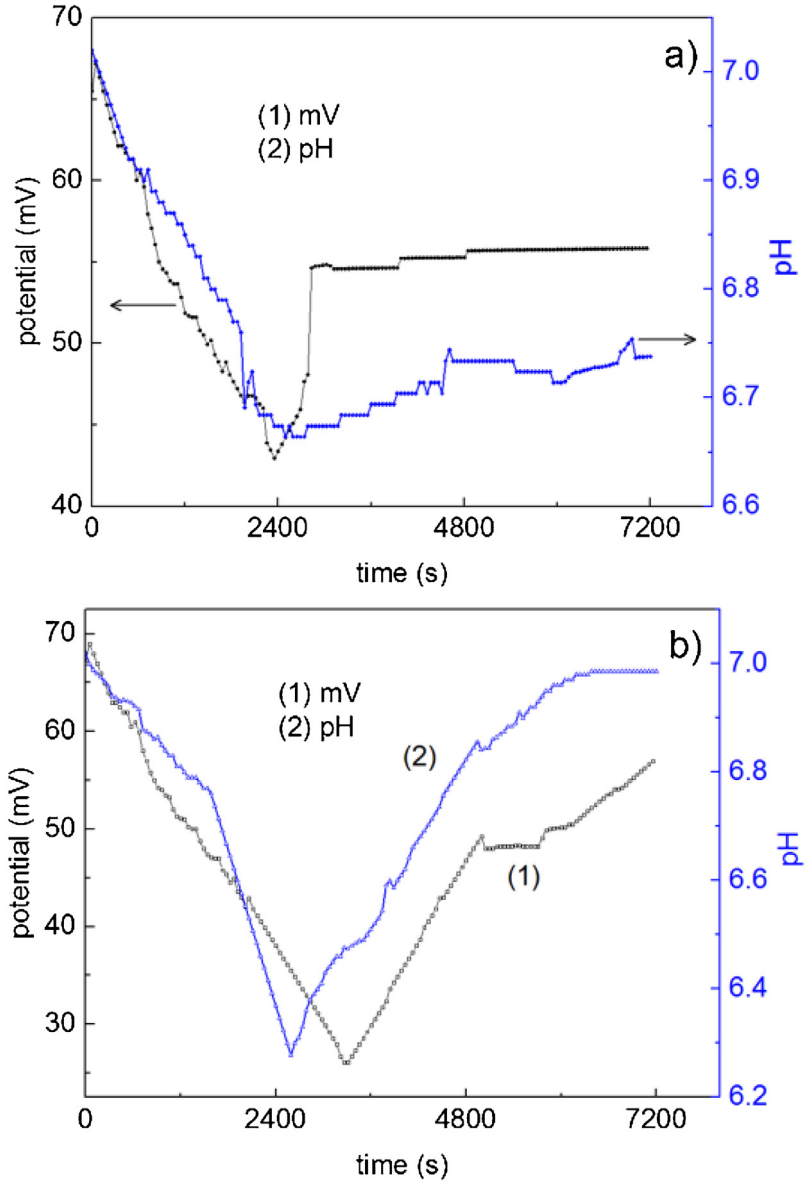

Fig. 4. (a) Interfacial potential and local-pH shifts of the bacterial culture contacted with TiO_2-ZrO_2-Cu in the dark within the bacterial inactivation time. (b) Interfacial potential and local pH shifts of the bacterial culture contacted with TiO_2-ZrO_2-Cu under light within the bacterial inactivation time. Suntest simulated light irradiation (50 mW/cm^2).

inactivation in aerobic conditions for TiO_2-ZrO_2 and TiO_2-ZrO_2-Cu PES films. The generation of OH•-radicals, HO_2°/O_2^{-} species and TiO_2-ZrO_2 vb(h+) holes under band-gap irradiation was shown in Fig. 2a/b and bacterial inactivation mechanism consistent with a pH-shift to more acidic values is suggested in reactions (1–6) below involving an unstable bacterial cationic species

$$\text{Bacteria} + [\text{PES-TiO}_2\text{-ZrO}_2] + \text{light} \rightarrow [\text{PES-TiO}_2\text{-ZrO}_2*]$$

$$\text{Bacteria} \rightarrow \text{Bacteria}^{+\cdot} + \text{PES-(TiO}_2\text{-ZrO}_2\text{)cbe}^{-} \quad (2)$$

$$\text{PES-(TiO}_2\text{-ZrO}_2\text{)cbe-} + \text{O}_2 + \text{H}^{+} \rightarrow \text{HO}_2^{\circ}\text{E}_0 - 0.05\text{NHE[23]} \quad (3)$$

$$\text{PES-(TiO}_2\text{-ZrO}_2\text{)cbe-} + \text{O}_{2\text{ads}} \rightarrow {}^{\circ-}\text{O}_{2\text{ads}}\text{E}_0 - 0.16\text{NHE[23]} \quad (4)$$

$$\text{PES-(TiO}_2\text{-ZrO}_2\text{)vbh}^{+} + \text{OH}^{-}{}_{\text{ads}} \rightarrow \text{OH}^{\bullet}\text{E}_0 - 1.90\text{NHE[3]} \quad (5)$$

$$\text{PES-(TiO}_2\text{-ZrO}_2\text{)vbh}^{+} + \text{H}_2\text{O}_{2\text{ads}} \rightarrow \text{OH}^{\bullet}{}_{\text{ads}} + \text{H}^{+} \quad (6)$$

$$\text{O}_2^{\circ-} + \text{H}^{+} \Leftrightarrow \text{HO}_2^{\circ}\text{pK}_a4.8$$

In Reaction (2), the HO_2° radical is stable at pH < 4.8, above this pH more than 50% is present in the form of $O_2^{\circ-}$ as noted in Reaction (6).

3.4. *Effect of the light dose on* E. coli *disinfection, repetitive bacterial inactivation and mechanistic considerations*

Fig. 5 shows the effect the light intensity applied to induce the bacterial inactivation mediated by TiO_2-ZrO_2-Cu and ZrO_2-TiO_2 films. Semiconductors like TiO_2 and ZrO_2 are affected by the incident light dose, but it is not known to what degree the Cu-intra-gap states are affected by the applied light dose [15]. Fig. 5, traces (1), (2) show similar bacterial inactivation kinetics under light doses of 50 mW/cm^2 and 70 mW/cm^2. This suggests a saturation effect by the bacterial culture for the incident photons. Fig. 5, trace (3) shows that when applying a light intensity <50 mW/cm^2, the kinetics becomes slower due to the lower number of surface charge carriers on the TiO_2-ZrO_2-Cu film. Cu on TiO_2-ZrO_2 accelerated the

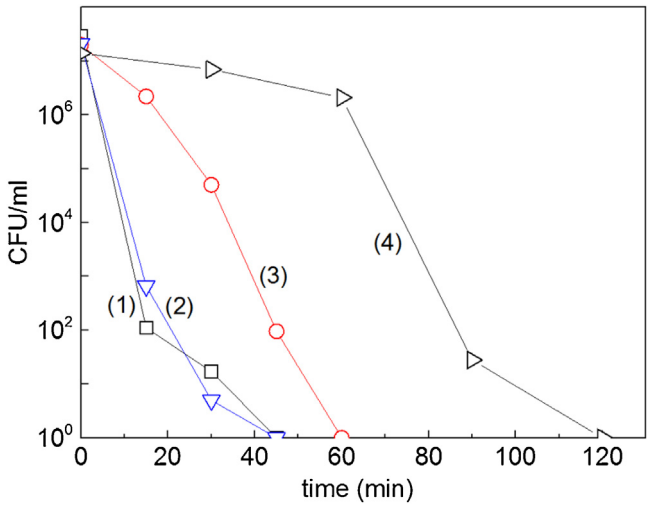

Fig. 5. *E. coli* inactivation by TiO_2-ZrO_2-Cu sputtered for 8 min/10 s under Suntest simulated solar light at three different light intensities as shown by traces: (1) 70 mW/cm^2 (2) 50 mW/cm^2 and (3) 30 mW/cm^2. For comparison purposes, trace (4) shows the bacterial inactivation on TiO_2-ZrO_2 under a light intensity of 50 mW/cm^2. Error bars: SD, σ = 5%.

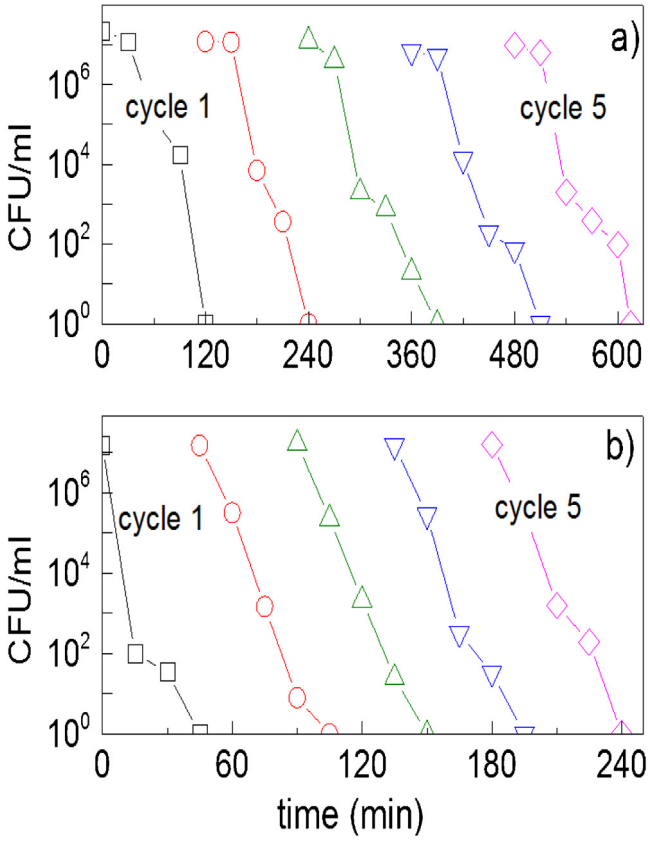

Fig. 6. (a) Recycling of TiO_2-ZrO_2 (8 min) and b) TiO_2-ZrO_2/Cu (8 min/10 s) under low intensity solar simulated light (50 mW/cm^2). Error bars: SD, σ = 5%.

bacterial inactivation kinetics. This is shown when comparing the bacterial inactivation kinetics in Fig. 5, trace (4) with the kinetics shown in Fig. 5, trace (1). The Cu intra-gap states/Cu-ions enhance electron-transfer and interact by electrostatic attraction with the negatively charged *E. coli* cell envelope. The Cu in ppb amounts has been reported to be highly toxic to bacteria [12,13,22,23].

Fig. 6a and Fig. 6b show the stable repetitive bacterial inactivation performance of the TiO_2-ZrO_2-Cu films. Fig. 6a shows the

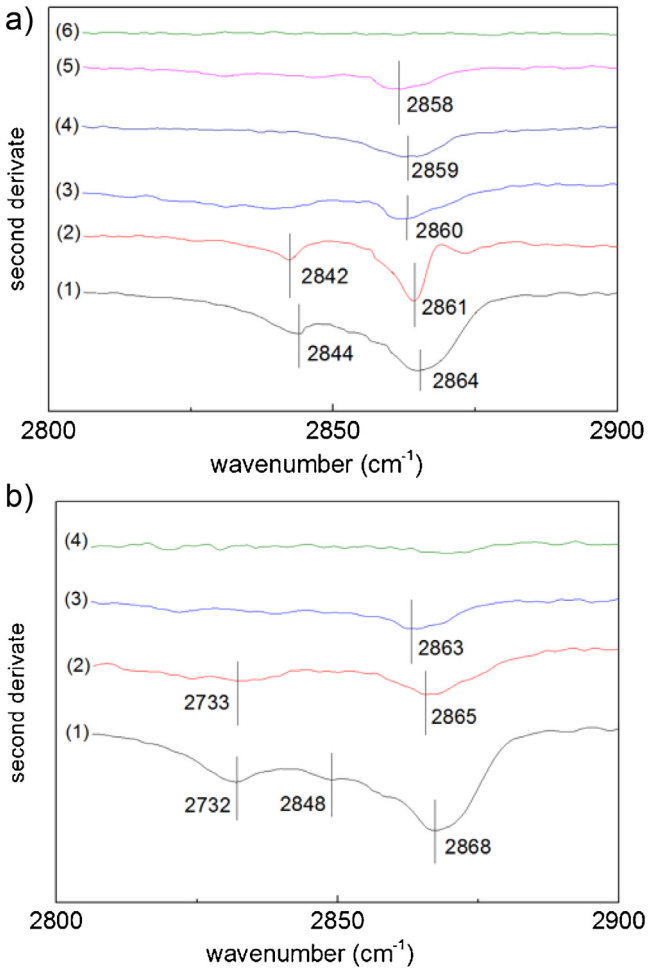

Fig. 7. a Shift in the $-CH_2$ vibrational peaks and amplitude changes during the bacterial inactivation of *E. coli* under light irradiation (50 mW/cm^2) followed by FTIR on TiO_2-ZrO_2 on PES at: (1) time zero, (2) after 15 min, (3) after 30 min, (4) after 60 min, (5) after 90 min and (6) after 120 min. (b) Shift in the $-CH_2$ vibrational peaks and amplitude changes during the bacterial inactivation of *E. coli* under light irradiation (50 mW/cm^2) followed by FTIR on TiO_2-ZrO_2-Cu on PES at: (1) time zero, (2) after 15 min, (3) after 30 min, (4) after 45 min.

bacterial inactivation induced by the ZrO_2-TiO_2 recycling up to the 5th cycle and Fig. 6b present similar runs mediated by ZrO_2-TiO_2-Cu films. No loss in activity was observed for either ZrO_2-TiO_2 or ZrO_2-TiO_2-Cu samples during the sample recycling. After each cycle the samples were thoroughly washed. These results show the potential for the application of binary-oxides decorated with Cu or not in disinfection processes.

3.5. FTIR spectroscopic changes observed within the time of bacterial inactivation

FTIR spectroscopy was used to monitor the shift in the symmetric stretching vibration peak $\nu_s(CH_2)$ photo-induced by the TiO_2-ZrO_2 and TiO_2-ZrO_2-Cu samples between 2800 and 2900 cm^{-1}. The FTIR-signals allowed the detection of the IR-spectral shifts and concomitantly the reduction of amplitude during bacterial inactivation. Fig. 7a shows the discontinuous IR-peak shift for methylene $\upsilon_s(\text{-}CH_2)$ from 2864 cm^{-1} at time zero up to 2858 cm^{-1} within 120 min, during bacterial inactivation on TiO_2-ZrO_2 PES. Fig. 7b presents the IR-shifts mediated by a TiO_2-ZrO_2-Cu showing the methylene $\upsilon_s(\text{-}CH_2)$ shift taking place at a faster pace within 45 min. The treatment of the IR data has been already reported, and therefore will not be addressed in detail in the present

study [24,25]. The shift peaks reflect an increasing C—C bond distance increasing with the time of irradiation introducing structural disorder in the outer lipo-polysaccharide layers (LPS) of *E. coli* [26,27]. This concomitant increased stretching leads to a more fluid LPS bilayer until the $-CH_2$-scission sets in after 120 min for TiO_2-ZrO_2 and after 45 min for TiO_2-ZrO_2-Cu in agreement with the bacterial inactivation times reported in Fig. 2a/b for both photocatalysts.

4. Conclusions

This study presents new evidence related to the bacterial inactivation/mineralization on TiO_2-ZrO_2 and TiO_2-ZrO_2-Cu films. *E. coli* inactivation on TiO_2-ZrO_2 and TiO_2-ZrO_2-Cu released ppb quantities of Ti, Zr and Cu. These quantities were below the toxicity limit set by sanitary regulations and suggest disinfection proceeding through an oligodynamic effect. The role of the decorated/intragap Cu on the mechanism of bacterial inactivation is a controversial matter and more work is necessary to clarify this issue. The shifts in local pH/interface potential during bacterial inactivation provide insight into the intermediates produced on the photocatalyst surface in the dark and under light. Disinfection in the dark only induced small changes in the pH/potential values within the period of bacterial inactivation compared to light activated reactions in aerobic conditions.

Acknowledgments

We thank the EPFL and Swiss National Science Foundation (SNF) Project (200021-143283/1) for financial support. We also thank the COST Action MP 1106 for discussions during the course of this study.

References

[1] G. Grass, C. Rensing, M. Solioz, Appl. Environ. Microb. 77 (2011) 1541–1547.
[2] Christophe Espiritu Santo, Ee Wen Lam, Christian G. Elowsky, Davide Quaranta, Dylan W. Domaille, Christopher J. Chang, Gregor Grass, Appl. Environ. Microb. 77 (2011) 794–802.
[3] Gadi Borkow, Jefferey Gabbay, Curr. Chem. Biol. 3 (2009) 272–278.
[4] H. Foster, I. Ditta, S. Varghese, A. Steele, Appl. Microb. Biotechnol. 90 (2012) 1847–1868.
[5] A. Fujishima, X. Zhang, D. Tryck, Surf. Sci. Rep. 63 (2008) 515–582.
[6] L. Zhang, R. Dillert, D. Bahnemann, M. Vormoor, Energy Environ. Sci. 5 (2012) 57491–57507.
[7] S. Rtimi, C. Pulgarin, R. Sanjines, V. Nadtochenko, J.-C. Lavanchy, J. Kiwi, ACS-Appl. Mater. Interface 7 (2015) 12832–12839 (and references therein).
[8] T. Busko, O. Dmytrenko, M. Kulish, Y. Prylutskyy, S. Shokhovets, G. Gobsch, V. Vityuk, A. Eremenko, V. Tkach, Mat. Wiss. u. Werkstofftech. 44 (2013) 119–122.
[9] Ch. Kim, H. Jeong, Bull. Korean Chem. Soc. 28 (2000) 2333–2336.
[10] E. Rentz, J. Nutr. Environ. Med. 13 (2003) 109–118.
[11] H.J. Jeng, J. Swanson, J. Environ. Sci. Health Part A Toxic Hazard. Subst. Environ. Eng. 4 (2006) 2699–2711.
[12] W. K. Nägeli, *Neue Denkschr. Allgeein. Schweiz. Gesellsch. Ges. Naturweiss. 1893, Bd XXXIII Abt 1*. English archive: Nägeli, *Denkschr. Allgemein. Naturfors Ges*, 33, 1983, 174–182.
[13] B. Stobie, B. Duffy, D. Mccormack, J. Colreavy, M. Hidalgo, P. Mchale, S. Hinder, Biomaterials 29 (8) (2008) 963–969.
[14] S. Banerjee, S. Pillai, P. Falaras, K. O'shea, J.-A. Byrne, D. Dionysiou, J. Phys. Chem. Lett. 5 (2014) 2543–2552.
[15] V. Etacheri, C. Di Valentin, J. Schneider, D. Bahnemann, S.C. Pillai, J. Photochem. Photobiol. 25 (2015) 1–29.
[16] J. Tauc, Mater. Res. Bull. 3 (1968) 37–46.
[17] S. Rtimi, C. Pulgarin, R. Sanjines, J. Kiwi, Appl. Catal. B 162 (2015) 236–244.
[18] A. Kraeutler, A. Bard, J. Am. Chem. Soc. 100 (1978) 239–2244.
[19] S. Sato, J. Phys. Chem. 87 (1983) 3531–3537.
[20] Z. Lu, Z.L. Zhou, Z. Zhang, W. Shi, Z. Xie, D. Pang, P. Shen, Langmuir 19 (2003) 8765–8768.
[21] S. Maheshwari, K. Singh, U. Minchita, R. Balakrishna, J. Photochem. Photobiol. A 88 (2012) 414–422.
[22] J. Schneider, M. Matsuoka, M. Takeuchi, J. Zhang, Y. Horiuchi, M. Anpo, D. Bahnemann, Chem. Rev. 114 (2014) 9919–9986.
[23] D.W. Synnott, M.K. Seery, S.J. Hinder, G. Michlits, S.C. Pillai, Appl. Catal. B 130–131 (2013) 106–111.
[24] S. Rtimi, R. Sanjines, M. Andrzejczuk, C. Pulgarin, A. Kulik, J. Kiwi, Surf. Coat. Technol. 254 (2014) 333–343.
[25] S. Rtimi, C. Pulgarin, R. Sanjines, J. Kiwi, RSC—Adv. 3 (2013) 16345–16348.
[26] J. Kiwi, V. Nadtochenko, J. Phys. Chem. B 108 (2004) 17675–17684.
[27] S. Rtimi, M.K.S. Ballo, D. Laub, C. Pulgarin, J. Entenza, A. Bizzini, R. Sanjines, J. Kiwi, Appl. Catal. A 498 (2015) 185–191.